DOI: 10.1002/zaac.201300336

Multi-shaped Amorphous Alloy Ni-B: Ultrasonically Aided Complexing-reduction Preparation, Catalytic Ability for $NaBH_4$ Hydrolysis Yielding H_2 Gas

Jun Zhang,[a] Chengxuan Li,[a] Lili Li,[a] Xigang Du,[a] Bangcai Song,[a] and Hang Xu[a]

Keywords: Amorphous materials; Alloys; Ni-B; Complexing reduction; $NaBH_4$; Hydrogen

Abstract. The multi-shaped amorphous alloy (Ni-B) powders were prepared by complexing reduction route using sodium borohydride ($NaBH_4$) as reductant with assistance of ultrasonic wave. The selected complexants, i.e. water, ammonia, salicylic acid, and ethylene diamine tetraacetic acid (EDTA) possess sequentially escalating complexation ability. The chemical composition and shapes of the product samples obtained under different conditions were characterized by X-ray powder differaction, selected area electron diffraction, and transmission electron microscope. The influence of reaction conditions such as the types of Ni-B, temperatures, $NaBH_4$ concentrations, and sodium hydroxide (NaOH) content on the hydrogen generation rate of hydrolysis of $NaBH_4$ solution were investigated in detail. The results show that the as-prepared Ni-B powders all belong to amorphous alloy with variable element contents, and the Ni-B sample prepared from EDTA complexation, possessing the best fineness and dispersity, has the strongest catalytic activity. The mean apparent activation energy of the hydrolysis reaction is 64.90 $kJ\cdot mol^{-1}$. The $NaBH_4$ concentration has little impact on hydrogen generation rate, implying that the catalytic hydrolysis of $NaBH_4$ solution should be the pseudo zero-order reaction. Keeping the NaOH content at below 5 % could inhibit the hydrolysis of $NaBH_4$ solution, but the NaOH contents from 10 % to 15 % will significantly promote the hydrolysis rate of $NaBH_4$. The hydrolysis reaction mechanisms, especially the effect of NaOH content on the hydrolysis reaction were also analyzed.

1 Introduction

Sodium borohydride ($NaBH_4$), a coordination hydride, is becoming an emerging and compelling hydrogen production material with high specific energy in recent years due to its high theoretical hydrogen storage of up to 10.6 wt %.[1] The hydrogen production by $NaBH_4$ hydrolysis possesses such advantages as high hydrogen gas purity, controllable gas release rate, high security, and recycling of byproduct, etc., already being used as the preferred hydrogen source of proton exchange membrane fuel cell (PEMFC). The hydrolysis of $NaBH_4$ in aqueous solution generates hydrogen gas and sodium hypoborate along with the heat release and the reaction rate is largely affected by temperature and pH value. Under the absence of catalysts, the relationship[2,3] among half-life period ($t_{1/2}$), temperature (T) and pH follows such an empirical formula: $\lg t_{1/2} = \text{pH}-(0.034T-1.92)$. The reaction half-life period could reach 400 d under normal temperature and higher pH value (pH>8), which is an appropriate reaction rate and can basically satisfy many actual applications. However, further studies confirm that heterogeneous catalytic hydrolysis of $NaBH_4$ solution should be more preferable in order to achieve quick start and controlled hydrogen evolution.

By now, the catalysts reported, which are suitable for hydrogen generation by $NaBH_4$ hydrolysis, are mainly noble metal ones, such as Pt[4,5] and Ru[6] with different supported form and loadings, as well as double noble metal catalysts loaded on $LiCoO_2$ surface[7]. Besides, some non-noble metal chlorides including $FeCl_2$, $CoCl_2$, $NiCl_2$[8], and Raney Ni, Raney Co, and relevant alloy Mg_xNi[9,10], etc., have also been intensively studied and used for the controllably catalytic hydrolysis of the borohydride. However, for catalysts mentioned above there more or less exist such shortcomings as high price, low activity, advance activation, unstable hydrogen releasing rate, and inconvenience of separation and regeneration, and so on. In contrast, amorphous alloy, which is endowed with distinguishing features of higher activity, lower cost, and easier recycling, has attracted lots of attention as a new type of catalyst in the last decades.

2 Experimental Section

2.1. Chemicals and Instruments

Nickel acetate [$Ni(CH_3COO)_2\cdot 4H_2O$], sodium borohydride ($NaBH_4$), sodium ethylene diamine tetraacetic acid ($C_{10}H_{14}N_2O_8Na_2\cdot 2H_2O$, EDTA), ammonia ($NH_3\cdot H_2O$), salicylic acid ($C_6H_4OHCOOH$) and sodium hydroxide (NaOH) are all analytically pure reagents and directly used without further purification. The phase state and chemical composition of the products were analyzed by X-ray powder diffractometer (XRD) (Advance-D8, Bruker, Germany) with Cu-K_α radiation (λ = 0.15406 nm) and inductively coupled plasma optical emission spectrometer (ICP-OES) (Optima 2100DV, Perkin–Elmer, US), respec-

---

* Prof. J. Zhang, Ph. D.
Fax: 86-379-64232193
E-Mail: j-zhang@126.com; zhjabc@mail.haust.edu.cn
[a] Chemical & Pharmaceutical Engineering School
Henan University of Science and Technology
263 Kaiyuan Avenue
Luoyang 471023, Henan Province, P. R.China

tively. Transmission electron microscopy (TEM) (H800, Hitachi, Japan) and scanning electron microscopy (SEM) (JSM-6330F, JEOL, Japan) were employed for the morphological observation and selected electronic diffraction measurement. The chemical valence states of elements on the surfaces of the Ni-B samples were determined with an X-ray photoelectron spectrometer (XPS) (PHI5400, Perkin-Elmer, US). A hermetically sealed magnetic stirring apparatus (Variomag, Thermo-Fisher, USA) was underwater placed in a waterbath to agitate the solution.

2.2 Preparation of Amorphous Alloy Ni-B Powders

A Ni^{2+} solution (20 mL, 0.2500 mol L^{-1}) was mixed with EDTA solution (20 mL, 0.1750 mol L^{-1}) whilst stirring, and the pH value of the mixture was adjusted to 3.5 through dropwise adding of HCl (4 mol L^{-1}). The resulting pale blue transparent solution was transferred into a flask, which in advance was put in 298 K water bath and ultrasonically treated (45 KHz, 100 W) for 30 min. Meanwhile, $NaBH_4$ (0.02 mol) was dissolved in a NaOH solution (10 mL, 0.01 mol L^{-1}), whose temperature was preset at about 273 K. Afterwards the alkaline $NaBH_4$ solution was added into the flask, and the reaction immediately started. Until no bubbles escape the reaction was terminated. The suspension liquid product was centrifuged, washed 3–5 times using water and absolute ethanol in turn and finally kept in absolute ethanol to avoid oxidation before use. The black solid powders separated by centrifugation should be vacuum dried at 333 K for 6 h, which was labeled as Ni-B-1.

Taking the similar tactic, through separately substituting salicylic acid, ammonia, and water for the above complexant EDTA, the corresponding black powders could also be obtained, which was sequentially labeled as Ni-B-2, Ni-B-3, and Ni-B-4.

2.3 The Evaluation method of Catalytic activity of Ni-B Samples

Into the $NaBH_4$ solution with a given concentration was added a certain amount of NaOH to maintain appropriate alkalinity, followed by the addition of the as-prepared Ni-B sample with different mass. The hydrogen generation volume in unit time from the hydrolysis reaction under different conditions was recorded in detail, so as to evaluate the catalytic activity of the corresponding Ni-B sample. In particular, a three-necked round-bottomed flask with proper capacity, equipped with a thermometer and a gas collecting device in the two side necks, respectively, was kept in a glassy thermostatic waterbath. A reasonable amount of catalyst Ni-B and alkaline $NaBH_4$ solution was successively added into the flask through the middle neck, and simultaneously agitated by a waterproof type magnetic stirrer. Once the reaction started, the hydrogen generation volumes in different time intervals should be accurately recorded.

Results and Discussion

3.1 Phase Analysis of As-prepared Amorphous Alloy Ni-B Powders

The phase structure of as-prepared Ni-B powders by using the given four complexants under different conditions was analyzed by X-ray powder diffraction, and the corresponding XRD pattern concerning Ni-B-1 was shown in Figure 1. The XRD pattern definitely displays only one wide-shoulder dispersion peak at around 45°(2θ), which belongs to the characteristic diffraction peak of amorphous alloy Ni-B.[11] No other impurity peaks appear, implying the relatively high purity of as-prepared Ni-B product. Moreover, further studies confirm that the XRD patterns of all the other Ni-B samples prepared under the given conditions were similar to Figure 1, indicating that the target product, namely amorphous alloy Ni-B, could be achieved according to the above experimental design. The other XRD patterns except that of Ni-B-1 are not shown herein for brevity.

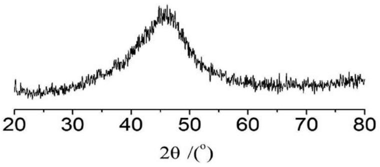

Figure 1. XRD pattern of Ni-B-1 amorphous alloy.

3.2 The Morphological Analysis of the Amorphous Alloy Ni-B Powders

The TEM images of Ni-B-1, Ni-B-2, Ni-B-3, and Ni-B-4 are displayed in Figure 2. It can be seen that Ni-B-1 particles, prepared by using the strongest complexant EDTA, have ball-like shape with average grain diameter of less than 40 nm. What is more, these particles possess good dispersity, relatively uniform size, clear interface, and hardly any aggregation. The morphology of Ni-B-2 particles is obviously different from that of Ni-B-1 due to adopting salicylic acid as complexant, whose complexing ability is weaker than EDTA. In this case, the particles with a little reunion are linked to each

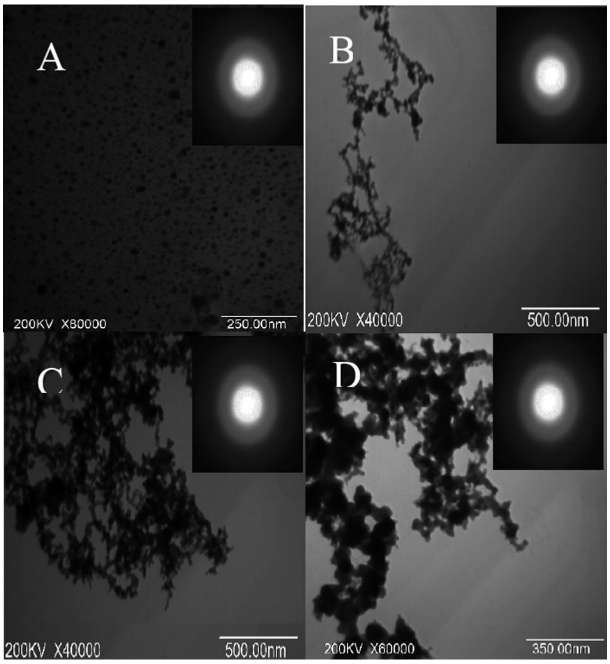

Figure 2. TEM and SAED images of Ni-B amorphous alloy: (A)Ni-B-1, (B)Ni-B-2, (C)Ni-B-3, (D)Ni-B-4.

other just like a line, and the average diameter increases to 70 nm. The complexing ability of ammonia further weakens, so its corresponding product, i.e. Ni-B-3 sample, is endowed with the reticular appearance, and with more serious aggregation and larger mean diameter of 100 nm. Among the four complexants the water has the weakest complexing ability, and its resulting Ni-B-4 sample shows much more serious aggregation and largest average diameter of 150 nm. The four inserted annular SAED images also verify the amorphous feature of the four kinds of Ni-B.

The reduction process of Ni^{2+} by $NaBH_4$ is a drastically exothermic reaction, and the reaction product Ni-B is at the thermodynamically metastable state.[12] The heat release during the reduction process could heat up the reaction system, intensifying the collision between the nascent product particles, and resulting in aggregation. On the other side, the formation of complex ions between complexant and Ni^{2+} ions inevitably cause the decrease of concentration of free Ni^{2+} in the solution, leading to slowdown of the reduction reaction rate, and weakening the collision and aggregation between nascent particles. The complexing ability or binding capacity of the complexants with Ni^{2+} successively declines in sequence of EDTA, salicylic acid, ammonia, and water, whose order is evidently in accordance with the agglomerate degree of Ni-B particles observed by TEM.

3.3 The Chemical Composition and Valence State of the Amorphous Alloy Ni-B Powders

The fresh Ni-B samples just separated from the absolute ethanol and dried in vacuo, were analyzed by ICP-AES and XPS, so as to determine chemical composition and valence state. The corresponding results are collected in Table 1. As can be found from Table 1, the nickel contents in the four Ni-B samples are slightly different, following such an ascending order from Ni-B-1, Ni-B-2, Ni-B-3, to Ni-B-4. This result could also be explained according to the aforesaid strong-to-weak sequence of the complexants. The XPS analysis results reveal that the average electron binding energy of Ni_{2p} in the Ni-B samples is 852.6 eV, coinciding basically with the standard electron binding energy of the metal nickel (852.3 eV). By comparison with the standard electron binding energy of B_{1s} in metalloid B (187.2 eV), it is easily found that each binding energy of B_{1s} in four Ni-B samples has shown positive shift. From Ni-B-1 to Ni-B-4, the positive shift values are 1.2 eV, 1.0 eV, 0.9 eV, and 0.3 eV, respectively, suggesting the evident existence of interaction between Ni and B atoms in the amorphous alloy Ni-B. Some of electrons in boron atoms transfer to nickel atoms, resulting in the formation of electron-rich nickel and electron-deficient boron in the alloy.[13] Based on the above experimental facts it is not difficult to judge that there should exist more electron transfers in the case of Ni-B-1.

Table 1. Atomic molar ratios and energy peaks of the Ni-B samples.

Atomic molar ratio		XPS energy peak /eV	
		B_{1s}	Ni_{2p}
Ni-B-1	$Ni_{73.6}B_{26.4}$	188.4	853.1
Ni-B-2	$Ni_{74.2}B_{25.8}$	188.2	852.7
Ni-B-3	$Ni_{74.9}B_{25.1}$	188.1	852.1
Ni-B-4	$Ni_{75.5}B_{24.5}$	187.5	852.5

3.4 The Evaluation of Catalytic Activity

3.4.1 The Catalytic Activity of the Different Ni-B Samples

The catalytic capacities of the different types of Ni-B samples were evaluated by the hydrolysis of $NaBH_4$ solution and the experimental results are shown in Figure 3. The hydrolysis reaction condition was designed as follows: reaction temperature 303 K, $NaBH_4$ concentration 0.0749 mol·L^{-1} (mass fraction 0.28 %), NaOH content 0.0100 mol·L^{-1} (mass fraction 0.04 %), and Ni-B dosage 0.6667 g·L^{-1}. As seen from Figure 3, within the first 20 min of the hydrolysis reaction, the hydrogen gas yield per unit time, i.e. hydrogen generation rate, catalyzed by Ni-B-1, Ni-B-2, Ni-B-3, and Ni-B-4, decreases sequentially. In comparison with those of Ni-B-2, Ni-B-3, and Ni-B-4, the hydrogen generation rate by using Ni-B-1 increases by 26 %, 43 % and 64 %, respectively. The required time that reaches a maximum hydrogen generation volume (35 mL) for Ni-B-1, Ni-B-2, Ni-B-3, and Ni-B-4 is quite different (20 min, 30 min, 40 min, and 60 min, respectively). If no any catalyst (Ni-B) was added, the $NaBH_4$ aqueous solution could only hydrolyze spontaneously, releasing only 1 mL hydrogen gas in 50 min, which stands in sharp contrast to that catalyzed by Ni-B powders. Theoretically, the catalytic activity of the Ni-B samples largely depends upon the number of active site of surface Ni atoms. Owing to unique microstructure of the amorphous alloy, the Ni atoms at electron-rich state could provide more active sites.[14] The XPS analysis results in Table 1 reveal that the enriching electron ability of Ni atoms in Ni-B-1, Ni-B-2, Ni-B-3, and Ni-B-4 successively decreases, and this sequence agrees with the catalytic activity of the Ni-B samples shown in Figure 3.

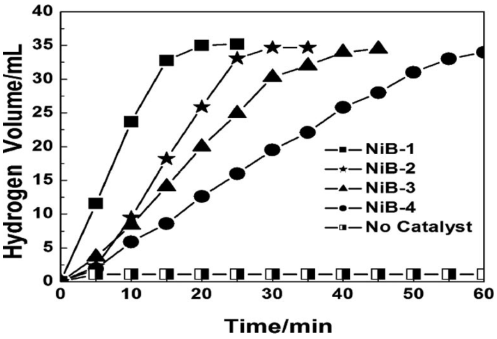

Figure 3. Hydrogen generation rate of $NaBH_4$ hydrolysis catalyzed by different Ni-B.

3.4.2 Effect of $NaBH_4$ Concentration on Hydrogen Yield

The Ni-B-1 sample, possessing the strongest catalytic activity among the four amorphous alloys, was used as catalyst to evaluate the effect of different $NaBH_4$ concentrations on hydrogen yield. Under such conditions as reaction temperature 303 K, NaOH content 0.0100 mol·L^{-1} and Ni-B-1 dosage 0.6667 g·L^{-1}, the hydrogen generation rate was investigated, and the results are shown in Figure 4. The hydrogen generation volume is 20 mL in the first 20 min reaction time, if the $NaBH_4$ concentration is kept at 0.28 % (mass fraction, the same below); similarly, in the same time span the hydrogen generation volume reaches 25 mL and 28 mL, respectively, as the $NaBH_4$ concentration rises up to 1 % and 5 %. These results indicate that in low content range (less than 5 %) the rising of $NaBH_4$ concentration could observably promote the hydrogen generation rate. However, while the $NaBH_4$ concentration continues to rise up to 10 % and 15 %, the hydrogen generation volumes within 20 min are only 29 mL and 30 mL, respectively, showing relatively smaller increments. On the whole, with the $NaBH_4$ concentration rising from 0.28 % to 15 %, the maximum hydrogen generation volume increases from 34.5 mL to 40.5 mL. In particular, the maximum hydrogen generation volume increases by only 1 mL when the $NaBH_4$ concentration increases from 5 % to 15 %. Figure 4 shows that the hydrogen generation rates under different $NaBH_4$ concentrations reveal very little variation in the same time, which corresponds to the kinetics feature of zero-order reaction[15]. As a reasonable inference, solubility of the byproduct ($NaBO_2$) from the hydrolysis reaction is 28.2 g at room temperature, which corresponds to the theoretical $NaBH_4$ concentration of 8.5 %.[16,17] Hence, under the higher $NaBH_4$ concentration (e.g. 5 %) the rapid hydrolysis reaction inevitably produces a mass of byproduct $NaBO_2$, meanwhile brings some water away along with the escape of H_2 gas. Such a double action will make $NaBO_2$ rapidly reach saturation point, and deposit on the surface of the catalyst, weakening the catalytic activity. On the other side, with the precipitation of $NaBO_2$, the hydrolysis solution becomes thicker and thicker, impeding the mass transfer, and further resulting in the decline of the hydrolysis reaction rate.

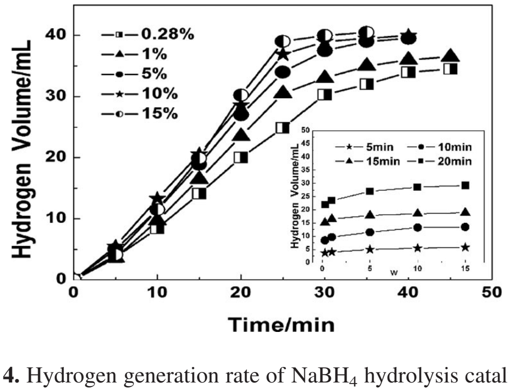

Figure 4. Hydrogen generation rate of $NaBH_4$ hydrolysis catalyzed by Ni-B-1 under different $NaBH_4$ concentrations.

3.4.3 Effect of Temperature on Hydrogen Yield

With the Ni-B-1 dosage and NaOH content in the solution kept at 0.6667 g·L^{-1} and 0.0100 mol·L^{-1}, respectively, the hydrogen generation capacity from hydrolysis of 0.0749 mol·L^{-1} $NaBH_4$ solution in the temperature range from 298 to 318 K were systematically studied. As shown in Figure 5, the hydrogen generation rates all increases with the rise of temperatures. Maximum hydrogen generation volume reaches 40 mL within 15 min at 318 K, while the maximal volume is only 5.5 mL at 298 K within the same time period. For the low temperatures less than 318 K, the maximum hydrogen generation volumes all decline in different degrees, in comparison with the results obtained at 318 K. Before reaching the maximum value, the hydrogen generation volumes at different temperatures linearly ascend with the hydrolysis time, but the variation of hydrogen generation volume tends to be flat after the maximum value. In addition, it also can be seen from Figure 5 that the hydrolysis reaction rate is relatively slow at 298 K. In the initial 5 min, there exists an induction period, which quickly disappears with the rise of temperature, and the reaction rate evidently speeds up after exceeding the induction period. As previously mentioned, the hydrolysis of $NaBH_4$ can be regarded as zero-order reaction, so the rate constant (k) can be calculated according to dynamics principle and equations. Based on Arrhenius equation, plotting ln(k) vs. the reciprocal of temperature (K), Figure 6 could be obtained. The apparent activation energy (E_a) could be calculated to be 64.9 kJ·mol^{-1}. Under the same conditions, the apparent activation energies of $NaBH_4$ hydrolysis catalyzed by Ni and CoB were reported to be 71 kJ·mol^{-1} and 68.87 kJ·mol^{-1},[18,19] respectively. By contrast, the apparent activation energy catalyzed by Ni-B-1 reduces by 6.1 kJ·mol^{-1} and 3.97 kJ·mol^{-1}, respectively.

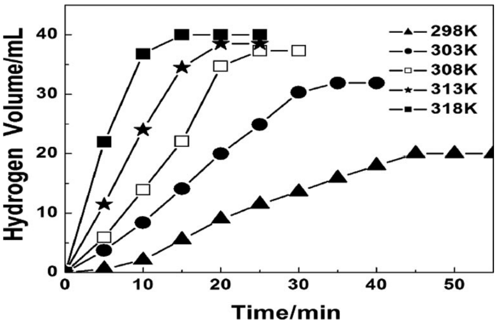

Figure 5. Hydrogen generation rate of $NaBH_4$ hydrolysis catalyzed by Ni-B-1 at different temperatures.

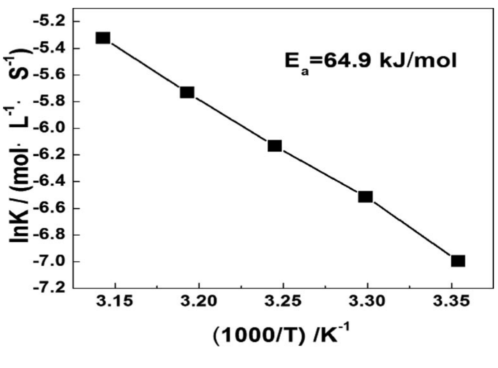

Figure 6. Plot of ln$k$ vs. 1/T for $NaBH_4$ hydrolysis catalyzed by Ni-B-1.

3.4.4 Effect of NaOH Concentration on Hydrogen Yield

With the Ni-B-1 dosage fixed at 0.6667 $g\cdot L^{-1}$, $NaBH_4$ concentration at 0.0749 $mol\cdot L^{-1}$ and hydrothermal temperature at 303 K, the hydrogen generation rates from $NaBH_4$ hydrolysis under different NaOH contents involving 0.04 %, 1 %, 5 %, 10 %, and 15 % were investigated. Just as seen from Figure 7, as the NaOH content is 0.04 % the hydrogen generation volume reaches 14 mL within 15 min, but the volume drops to only 6 mL, while the NaOH content is 1 %. Furthermore, continuing to elevating the NaOH content to 5 % results in the bigger decline of hydrogen generation volume, that is, dropping to 2.5 mL. However, the hydrogen generation rate dramatically increases to 27.7 mL per 15 min if the NaOH content rises to 10 %. In the case of 15 % NaOH content, the hydrogen generation rate is 27 mL per 15 min, almost remaining unchanged, compared with 10 % NaOH content. The above experimental results clearly show that the role of NaOH not only promote but also inhibit the hydrolysis reaction, and the NaOH content seems to have a strange "threshold".

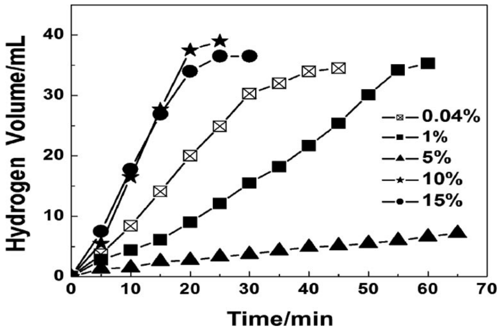

Figure 7. Hydrogen generation rate of $NaBH_4$ hydrolysis catalyzed by Ni-B-1 under different NaOH contents.

The influencing mechanisms of NaOH concentration on catalytic hydrolysis of $NaBH_4$ solution must be quite complex, and different explanations were suggested elsewhere.[20,21] Based on the above experimental results, the following two-step reaction mechanisms are here proposed: $BH_4^- + H_2O \rightarrow BH_3 + H_2(g) + OH^-$ (I); $BH_3 + OH^- + H_2O \rightarrow BO_2^- + 3H_2(g)$ (II). When NaOH concentration is lower than the threshold, reaction (I) should be the control step for the whole hydrolysis process; increasing the concentration of OH^- is not in favor of the reaction (I) and thus inhibit the whole hydrolysis reaction. Otherwise, if the NaOH concentration is higher than the threshold, the reaction (II) may dominate the hydrolysis process; increasing the concentration of OH^- should benefit reaction (II) and significantly improve the hydrogen generation rate. Theoretically, the molar quantity of hydrogen generation of reaction (II) should be three times of that of the reaction (I).

On the other side, the rapid development of reaction (II) inevitably leads to the formation and aggregation of the byproduct $NaBO_2$, which has small solubility in the aqueous solution. The precipitation of $NaBO_2$ on surface of the catalyst particles would decrease mass transfer, and impair catalytic activity. On basis of the above analysis from the both aspects, it is not difficult to infer that the hydrogen generation rate gradually declines prior to the "threshold" (e.g. 5 %) of the NaOH concentration. However, after exceeding the "threshold" concentration, the hydrogen generation rate shows a significant rise. Therefore, the two-step reaction mechanism could provide a reasonable explanation for the action of NaOH.

4 Conclusions

The four kinds of amorphous alloy (Ni-B-1, Ni-B-2, Ni-B-3, and Ni-B-4) were prepared by ultrasonically assisted complexing-reduction approach using EDTA, salicylic acid, ammonia, and water as complexants. Through the characterization and catalytic activity evaluation for these Ni-B samples, it could be concluded: (1) The as-prepared Ni-B samples were verified to be all non crystal matters. The complexing ability largely affects the chemical composition and phase state of the Ni-B products. The stronger the complexing ability of the complexant is, the smaller the Ni-B particle size is, the higher the dispersity is. (2) With EDTA used as complexant, the resulted product Ni-B-1 has the highest catalytic capacity for the hydrogen production from $NaBH_4$ hydrolysis. Compared with Ni-B-2, Ni-B-3, and Ni-B-4, not only the hydrogen generation volume from $NaBH_4$ hydrolysis catalyzed by Ni-B-1 within 20 min increases by 26 %, 43 %, and 64 %, respectively, but also it reaches the maximum hydrogen generation volume in the first place. (3) Increasing the reaction temperature benefits the rising of the hydrolysis reaction rate. The apparent activation energy of the hydrolysis reaction is calculated to be 64.90 $kJ\cdot mol^{-1}$. (4) The $NaBH_4$ concentration has little influence on the hydrogen generation rate, inferring to the chemical kinetics characteristics of zero-order reaction. (5) Keeping the NaOH content less than 5 % will inhibit the hydrolysis of $NaBH_4$, while maintaining the NaOH content at 10 % to 15 % will dramatically promote the hydrogen generation rate.

Acknowledgements

The authors gratefully acknowledge the financial support from the National Natural Science Foundation of China (21076063, 21006057), Henan Provincial Development Foundation for Science and Technology (102102210170), Project for Development of Science and Technology of Luoyang (1101030A), the Key Laboratory Construction Project for Chemical Engineering of Mineral Resources of Luoyang (1003016A).

References

[1] X.-M. Pan, J.-X. Ma, *Natural Gas Chem. Ind.* **2003**, *28*, 51–55.
[2] T. Wang, X.-G. Zhang, J. Li, *J. Fuel Chem. Technol.* **2004**, *32*, 723–728.
[3] D.-Y. Xu, H.-M. Zhang, W. Ye, *Prog. Chem.* **2007**, *19*, 1598–1605.
[4] Y. Kojima, K. Suzuki, K. Fukumoto, *Int. J. Hydrogen Energy* **2002**, *27*, 1029–1034.
[5] C. Wu, H.-M. Zhang, B.-L. Yi, *Catal. Today* **2004**, *93–95*, 477–483.
[6] S. C. Amendola, S. L. Sharp-Goldman, M. S. Janjua, *Int. J. Hydrogen Energy* **2000**, *25*, 969–975.

[7] P. Krishnan, T. H. Yang, W. Y. Lee, *J. Power Sources* **2005**, *143*, 17–23.
[8] B. H. Liu, Z. P. Li, *J. Alloys Compd.* **2006**, *415*, 288–293.
[9] R. Fernandes, N. Patel, A. Miotello, *Appl. Catal. B: Environ* **2009**, *92*, 68–74.
[10] Z. B. Yu, M. H. Qiu, H. X. Li, *Appl. Catal. A: Gen.* **1997**, *163*, 1–13.
[11] L. Damjanović, S. Bennici, A. Auroux, *J. Power Sources* **2010**, *195*, 3284–3292.
[12] A. J. Frierdich, C. E. Joseph, T. J. Strathmann, *Appl. Catal. B: Environ.* **2009**, *90*, 175–183.
[13] Y. Zhu, F. Liu, W. Ding, X. Guo, *Angew. Chem. Int. Ed.* **2006**, *45*, 7211–7214.
[14] H. Dong, H. X. Yang, *Int. J. Hydrogen Energy* **2003**, *28*, 1095–1100.
[15] P. Zhao, Z. Xie, *Power Technol.* **2007**, *31*, 988–990.
[16] C. M. Kaufman, B. Sen, *J. Chem. Soc. Dalton Trans.* **1985**, *93*, 307–313.
[17] S. U. Jeong, R. K. Kim, E. A. Cho, *J. Power Sources* **2005**, *144*, 129–134.
[18] A. M. F. R. Pinto, D. S. Falcão, *Int. J. Hydrogen Energy* **2006**, *31*, 1341–1347.
[19] G. C. Guella, Z. B. Patton, A. Miotello, *J. Phys. Chem. B* **2006**, *110*, 17024–17033.
[20] R. S. Liu, H. C. Lai, N. C. Bagkar, *J. Phys. Chem. B* **2008**, *112*, 4870–4875.
[21] Q. L. Zhang, Y. Wu, X. L. Sun, *Ind. Eng. Chem. Res.* **2007**, *46*, 1120–1124.

Received: July 9, 2013